

π bonding abilities is in progress and will provide definite answers regarding the importance of the Cornwell-Santry effect in the spin-paired d^6 transition-metal complexes.

Acknowledgment. We are grateful to Professor M. B. Celap for helpful discussions and to M. J. Malinar, who kindly supplied some of the complexes. This work was supported by funds from NIH Grant GM-21148 and by PSC-CUNY Research Awards 13118 and 12280 to R.L.L., who thanks Sandoz, Inc., for its hospitality during part of the preparation of this manuscript.

Appendix

The paramagnetic shielding term in a molecular orbital description has the following form:¹⁹

$$\sigma_{\alpha\alpha}^p = -2\beta^2 \sum_n (E_n - E_0)^{-1} \left[\left\langle \psi_0 \left| \sum_k \frac{l_{\alpha,k}}{r_k^3} \right| \psi_n \right\rangle \left\langle \psi_n \left| \sum_j l_{\alpha,j} \right| \psi_0 \right\rangle + CC \right] \quad (A1)$$

For cobalt(III) complexes with octahedral ligand field symmetry, paramagnetic shielding arises from the ${}^1A_{1g} \rightarrow {}^1T_{2g}$ transition,¹³ and expression A1 can be reduced to

$$\sigma_{\alpha\alpha}^p = \frac{8\beta^2}{\Delta E({}^1A_{1g} \rightarrow {}^1T_{2g})} \left\langle \psi_{t_{2g}} \left| \frac{l_{\alpha}}{r^3} \right| \psi_{e_g} \right\rangle \left\langle \psi_{e_g} \left| l_{\alpha} \right| \psi_{t_{2g}} \right\rangle \quad (A2)$$

$\alpha \in x, y, z$

Expression A2 is the basis for calculating the shielding of a nucleus directly bonded to cobalt(III). Molecular orbitals ψ_{e_g} and $\psi_{t_{2g}}$ are expressed as linear combinations of metal and ligand atomic orbitals. The paramagnetic term is calculated following the procedure of Cornwell.¹⁵ Thus, for operator l/r^3 all terms are dropped except those on the atom for which σ^p is sought. We chose to calculate the shielding on a ligator in position 5 (see Figure 5), so that only excitations along the x and y axes of the complex contribute to σ^p , i.e.,

$$\sigma_{av}^p = \frac{1}{3} (\sigma_{xx}^p + \sigma_{yy}^p)$$

Because $\psi_{t_{2g}}$ and ψ_{e_g} are antibonding orbitals, shielding along the y axis is

$$\sigma_{yy}^p(5) = -\frac{8\beta^2}{\Delta E} \left\langle \psi_{z^2}^a \left| \frac{l_y}{r^3(5)} \right| \psi_{xz}^a \right\rangle \left\langle \psi_{xz}^a \left| l_y \right| \psi_{z^2}^a \right\rangle \quad (A3)$$

where (see Figure 5)

$$\psi_{z^2}^a = a_{\sigma} d_{z^2} - \frac{b_{\sigma}}{2\sqrt{3}} (p_x^{(1)} + p_y^{(2)} - p_x^{(3)} - p_y^{(4)} - 2p_z^{(5)} + 2p_z^{(6)})$$

$$\psi_{xz}^a = a_{\pi} d_{xz} - \frac{b_{\pi}}{2} (p_z^{(1)} - p_z^{(3)} + p_x^{(5)} - p_x^{(6)})$$

For operator l_y it is necessary to keep the terms on all atoms. However, if overlap effects are neglected local origins are properly used for l_y and a good estimation may be obtained by considering only local terms.¹⁵ With this procedure it follows that

$$\left\langle \psi_{z^2}^a \left| \frac{l_y}{r^3(5)} \right| \psi_{xz}^a \right\rangle = i \frac{b_{\sigma} b_{\pi}}{2(3)^{1/2}} \langle r^{-3} \rangle_L \quad (A4)$$

where $\langle r^{-3} \rangle_L$ is the mean reciprocal cubic distance of ligator p electrons from the ligator nucleus. The same values are obtained for shielding along the x axis so that additional shielding of the ligator nucleus from the Cornwell-Santry effect is given by

$$\sigma_{av}^p(L) = \frac{8\beta^2}{3} \frac{\langle r^{-3} \rangle_L}{\Delta E} b_{\sigma} b_{\pi} \left(a_{\sigma} a_{\pi} - \frac{1}{2} b_{\sigma} b_{\pi} \right) \quad (A5)$$

Registry No. 1, 13408-73-6; **2,** 14408-57-2; **3,** 57298-57-4; **4,** 57335-06-5; **5,** 17439-00-8; **6,** 30364-77-3; **7,** 14320-09-3; **8,** 21520-57-0; **9,** 36527-85-2; **10,** 65816-56-0; **11,** 16986-03-1; **12,** 71926-48-2; ¹⁵N, 14390-96-6.

Solution Structure of Tris[hydridotris(pyrazol-1-yl)borato]ytterbium(III): Rare Example of Solution Rigid Lanthanide Complex

Matthew V. R. Stainer* and Josef Takats*

Contribution from the Department of Chemistry, The University of Alberta, Edmonton, Alberta, Canada T6G 2G2. Received June 11, 1982

Abstract: The ¹H, ¹³C, and ¹¹B NMR spectra of Lu(HBPz₃)₃ and Yb(HBPz₃)₃ (Pz = pyrazolyl, C₃N₂H₃) complexes have been recorded. The complexes are stereochemically rigid on the NMR scale with solution structure approximating the known solid-state structure of Yb(HBPz₃)₃. The molecules have C₃ symmetry in solution, and accordingly, the ytterbium complex gives rise to 21, 18, and 3 well-separated and lanthanide-shifted resonances in the ¹H, ¹³C, and ¹¹B NMR spectrum, respectively. Least-squares fits of the lanthanide-induced shifts in the paramagnetic Yb(HBPz₃)₃ complex to the solid-state structural data, using the full form of the McConnell-Robertson expression for the dipolar shifts, gave the molecular susceptibility anisotropies of the complex and the orientation of the magnetic axes in the complex. The C₃ molecular symmetry fixes the z magnetic axis perpendicular to the mirror plane, while the magnetic x axis refines to a position close to the pseudo-C₂ axis of the coordination polyhedron, which has approximate C_{2v} symmetry. The close agreement between calculated dipolar shifts and experimentally observed lanthanide-induced shifts confirms that the solid-state molecular structure remains essentially unchanged on dissolution and shows that contributions to the induced shifts in the ytterbium complex by a Fermi contact mechanism are minimal.

In the course of our studies on lanthanide complexes containing the potentially tridentate HBPz₃⁻ (Pz = pyrazolyl, C₃N₂H₃) ligand, we prepared the tris[hydridotris(pyrazol-1-yl)borato]lanthanide complexes, Ln(HBPz₃)₃.¹ An X-ray structure determination²

of the ytterbium complex revealed that the complex is eight-coordinate, with one free uncoordinated pyrazolyl group directed away from the metal center in a fashion which appeared to preclude its participation in an intramolecular ligand exchange

(1) Bagnall, K. W.; Tempest, A. C.; Takats, J.; Masino, A. P. *Inorg. Nucl. Chem. Lett.* 1976, 12, 555.

(2) Stainer, M. V. R.; Takats, J. *Inorg. Chem.* 1982, 21, 4044.

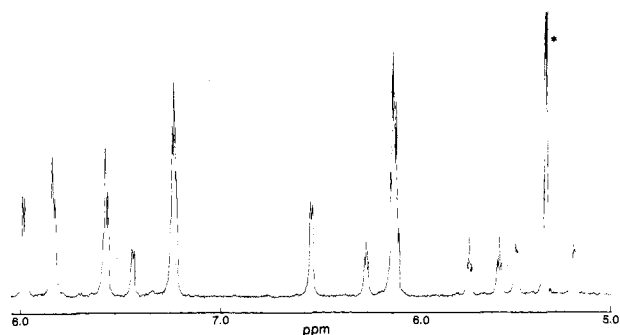


Figure 1. 200-MHz ^1H NMR spectrum of $\text{Lu}(\text{HBPz}_3)_3 \cdot \text{CH}_2\text{Cl}_2$.

process. Since paramagnetic lanthanide ions have been used extensively as probes in determining molecular structure and conformation of lanthanide-bound ligands in solution,³ it was of interest to determine whether the presence of such a probe in the complex could be used successfully to elucidate the solution structure of the molecule. In this paper we report on the solution ^1H , ^{13}C , and ^{11}B NMR studies of the $\text{Lu}(\text{HBPz}_3)_3$ and $\text{Yb}(\text{HBPz}_3)_3$ complexes. Surprisingly, the investigation revealed that the molecules are rigid in solution. It will be shown also that the lanthanide-induced shifts (LIS) in the ytterbium complex are well accounted for by using the solid-state structure of $\text{Yb}(\text{HBPz}_3)_3$ ² and the general form of the equation for dipolar shifts (vide infra).

Experimental Section

$\text{Yb}(\text{HBPz}_3)_3$ and $\text{Lu}(\text{HBPz}_3)_3$ were prepared by a previously reported procedure.¹ All NMR spectra were recorded with a Bruker WH-200 spectrometer. The probe temperature was 25 °C. The 200-MHz ^1H spectra were recorded by using 5-mm sample tubes and CD_2Cl_2 solvent. The 50.33-MHz ^{13}C and 64.23-MHz ^{11}B spectra were recorded by using a multinuclear probe and a 20-mm sample tube fitted with a vortex plug. The solvent was CH_2Cl_2 with 10% CD_2Cl_2 . The volume of the sample was typically 12 mL and sample concentrations were ~ 0.08 M. CH_2Cl_2 and CD_2Cl_2 were dried and distilled from P_2O_5 . Chemical shifts in the ^1H and ^{13}C spectra were measured with respect to internal standards: CH_2Cl_2 , δ 5.32, and CH_2Cl_2 , δ 53.8, respectively. The ^{11}B shifts were measured relative to external $\text{BF}_3\cdot\text{OEt}_2$ and were corrected for bulk magnetic susceptibility effects. The chemical shifts in this work are reported with respect to Me_4Si or $\text{BF}_3\cdot\text{OEt}_2$; downfield shifts are positive.

Results and Discussion

The ^1H NMR spectrum of $\text{Lu}(\text{HBPz}_3)_3$ is shown in Figure 1 and the chemical shifts are detailed in Table I. The spectrum of the diamagnetic complex, although more complicated, corresponds to that of the free HBPz_3^- ligand.⁴ The 3-H and 5-H protons appear as doublets ($J = 2$ Hz) mostly between δ 6.5 and 8.0 and the 4-H protons as triplets ($J = 2$ Hz) between δ 5.5 and 6.5. The ^{13}C NMR spectrum of $\text{Lu}(\text{HBPz}_3)_3$ is also listed in Table I. The 3- and 5-carbons are found between 134 and 144 ppm and the 4-carbons between 103 and 105 ppm downfield from Me_4Si . The shifts are similar to those found for pyrazole and the HBPz_3^- ligand.⁵ The carbons of the pyrazolyl rings exhibit a coupling of ~ 180 Hz with the proton to which they are bonded. The ^{11}B spectrum shows a single resonance at -4.1 ppm relative to $\text{BF}_3\cdot\text{OEt}_2$. By comparison the ^{11}B nuclei in $\text{Zn}(\text{HBPz}_3)_2$ ⁶ and KHBPz_3 ⁴ appear at -4.9 and -1.5 ppm, respectively. The complicated nature of the $\text{Lu}(\text{HBPz}_3)_3$ ^1H and ^{13}C NMR spectra suggests that the structure in solution is one of low symmetry which is not rapidly rearranging by either intramolecular or intermolecular exchange processes.

(3) (a) Sievers, R. E., Ed. "Nuclear Magnetic Resonance Shift Reagents"; Academic Press: New York, 1973. (b) Horrocks, W. DeW. In "NMR of Paramagnetic Molecules"; LaMar, G. N., Horrocks, W. DeW., Holm, R. H., Eds.; Academic Press: New York, 1973; p 479. (c) Dobson, C. M.; Levine, B. A. In "New Techniques in Biophysics and Cell Biology"; Pain, R. H., Smith, B. J., Eds.; Wiley: London, 1974; p 61. (d) Morris, A. T.; Dwek, R. A. *Quart. Rev. Biophys.* **1978**, *10*, 421.

(4) Trofimenko, S. *J. Am. Chem. Soc.* **1967**, *91*, 3170.

(5) Bagnall, K. W.; Edwards, J.; Heatley, F. In "Transplutonium Elements"; Müller, W., Lindner, R., Eds.; North-Holland Publishing Co.: Amsterdam, Holland, 1976; p 119.

(6) Jesson, J. P.; Trofimenko, S.; Eaton, D. R. *J. Am. Chem. Soc.* **1967**, *89*, 3148.

Table I. ^1H , ^{13}C , and ^{11}B Chemical Shifts of $\text{Lu}(\text{HBPz}_3)_3$ ^a

^1H	^{13}C	^{11}B
7.92 d (2)	143.45 (2)	-4.1
7.79 m (3)	142.16 (1)	
7.52 m (3)	141.92 (2)	
7.38 d (1)	141.73 (1)	
7.19 m (3)	141.02 (2)	
6.49 d (2)	138.42 (1)	
6.22 t (1)	136.92 (1)	
6.07 m (3)	136.43 (4)	
5.70 t (1)	133.93 (2)	
5.55 t (1)	132.84 (1)	
5.47 d (1)	132.56 (1)	
5.18 d (1)	105.32 (2)	
	104.67 (2)	
4.5 vb (3)	104.45 (3)	
	103.72 (1)	
	103.36 (1)	

^a d = doublet, t = triplet, m = multiplet, vb = very broad; relative intensities in parentheses.

The ^1H NMR spectrum of $\text{Yb}(\text{HBPz}_3)_3$ is shown in Figure 2. The most striking features of the spectrum are its complex nature and the large lanthanide-induced shifts caused by the paramagnetic ytterbium ion. The range in the chemical shifts is ~ 200 ppm. Inspection of the spectrum reveals that the 30 ^1H nuclei in the complex give rise to only 21 resonances (18 from the pyrazolyl protons and 3 from the B-H protons). Similarly the ^{13}C NMR spectrum has 18 resonances with the same intensity distribution as the signals arising from the pyrazolyl protons, 9 resonances of relative intensity 2 and 9 resonances of relative intensity 1. The ^{11}B spectrum, Figure 3, has three well-separated resonances integrating with a 1:1:1 ratio. The number and relative intensities of the signals indicate the presence of a mirror plane in the solution structure which causes the equivalence of six pyrazolyl rings in a pairwise fashion while maintaining the other three and the boron atoms distinct. Reference to Figure 4 shows that only a slight modification of the approximate C_3 solid-state structure of the molecule is required to account for the solution NMR features. It may be concluded therefore that the solution structure of $\text{Yb}(\text{HBPz}_3)_3$ is very close to its solid-state structure and perhaps more intriguingly the molecule is stereochemically rigid on the NMR time scale. This last observation is rather surprising and was certainly not the expected outcome of the investigation. Eight-coordinate complexes are almost invariably highly nonrigid, and only in rare cases did low-temperature NMR studies reveal stoppage of the rearrangement and allow the successful recording of the limiting static spectrum of the molecules.^{7,8} Lanthanide complexes are known to be highly labile both toward intramolecular and intermolecular exchange processes. Rigidity at or near room temperature has been observed only recently with highly constrained crown ether type ligands⁹ and a macrocyclic nitrogen ligand.¹⁰ As detailed in the structural paper,² we believe that the fortuitous ligand wrapping of the HBPz_3^- ligand system is responsible for the solution rigidity of the present complexes. Whatever the exact reasons for this behavior, the rigidity of the structure, the known solid-state structure, and the presence of a large number of distinct NMR nuclei all conspire to make $\text{Yb}(\text{HBPz}_3)_3$ an especially interesting complex with regard to NMR studies of lanthanide complexes.

Starting with the twin assumptions that the structure observed in the solid state is maintained in solution and that in the ^1H NMR spectrum Fermi contact contributions to the LIS will be negli-

(7) (a) Fay, R. C.; Lewis, D. F.; Weir, J. R. *J. Am. Chem. Soc.* **1975**, *97*, 7179; $[\text{Ta}(\text{S}_2\text{CNMe}_2)_4]^+$. (b) Fay, R. C.; Howie, J. K. *J. Am. Chem. Soc.* **1972**, *99*, 8110; $\text{Zr}(\text{acac})_4$ and $\text{U}(\text{acac})_4$.

(8) Donahue, C. J.; Archer, R. D. *J. Am. Chem. Soc.* **1977**, *99*, 6613; tris(5-methylpicolinato)(5,7-dichloro-8-quinolinato)tungsten(IV), first example of rigidity for $\text{M}(\text{chelate})_4$ above room temperature.

(9) (a) Catton, G. A.; Harman, M. E.; Hart, F. A.; Hawkes, G. E.; Moss, G. P. *J. Chem. Soc., Dalton Trans.* **1978**, 181. (b) Gansow, O. A.; Pruett, D. J.; Triplett, K. B. *J. Am. Chem. Soc.* **1979**, *101*, 4408.

(10) Desreux, J. F. *Inorg. Chem.* **1980**, *19*, 1319.

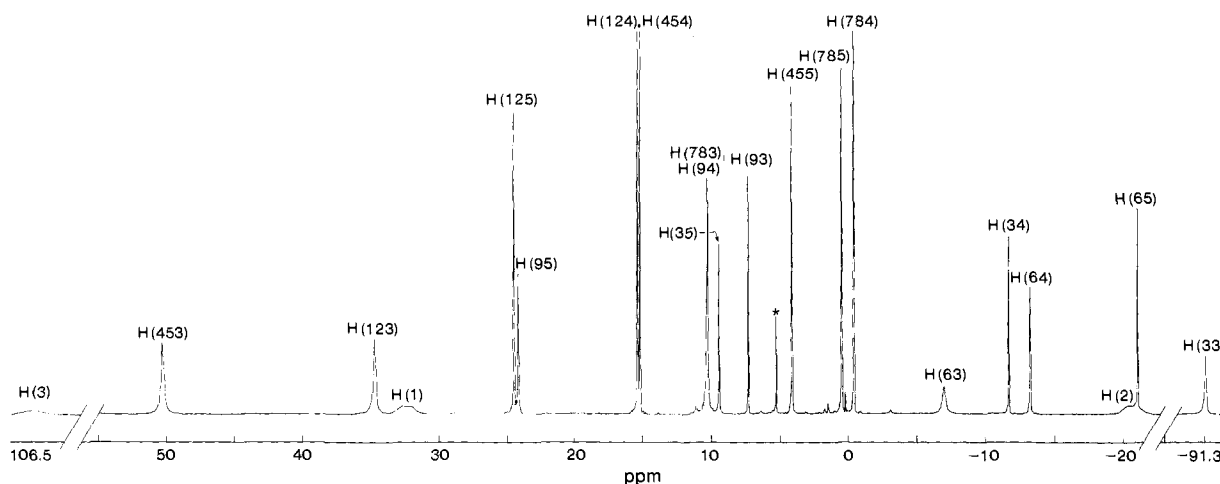


Figure 2. 200-MHz ^1H NMR spectrum of $\text{Yb}(\text{HBPz}_3)_3$ at 298 K, $^*\text{CH}_2\text{Cl}_2$; for assignment and numbering scheme, see text.

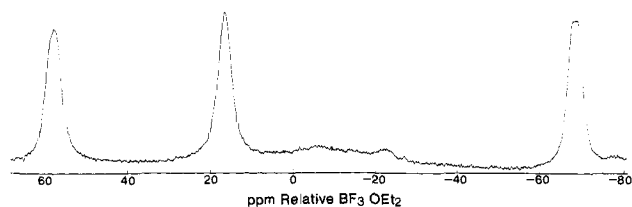


Figure 3. 64.23-MHz ^{11}B NMR spectrum of $\text{Yb}(\text{HBPz}_3)_3$.

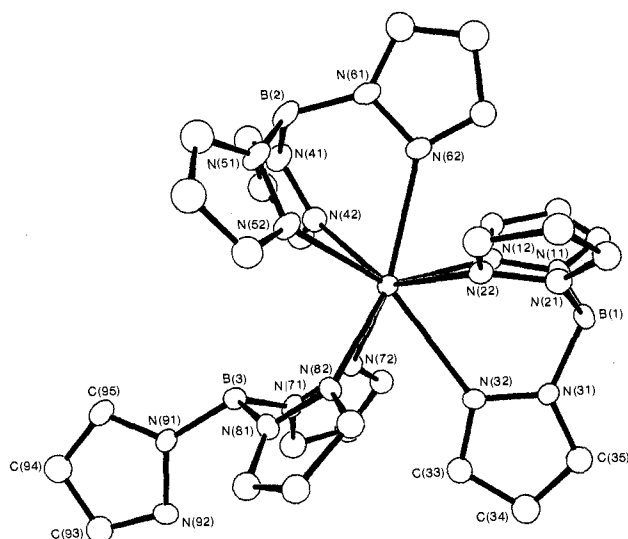


Figure 4. Perspective view of the solid-state structure of $\text{Yb}(\text{HBPz}_3)_3$ perpendicular to the approximate molecular mirror plane. The atom numbering scheme is shown also.

gible,¹¹ we attempted a fit of the observed lanthanide-induced shifts to calculated dipolar shifts. The rigidity and absence of axial symmetry of the solution structure requires the use of the full McConnell–Robertson equation¹³ for the calculation of the dipolar shifts, $(\Delta\nu/\nu_0)\text{dip}$. Theoretical work has shown that this equation can be expressed in terms of magnetic susceptibilities^{12b,14}

$$\left(\frac{\Delta\nu}{\nu_0}\right)\text{dip} = D_1 \frac{(3 \cos^2 \theta - 1)}{r^3} + D_2 \frac{\sin^2 \theta \cos 2\Omega}{r^3} \quad (1)$$

(11) This is a valid assumption since it is known that amongst the lanthanides $\text{Yb}(\text{III})$ exhibits the largest relative dipolar contribution to LIS; contact contribution appears to be negligible.¹²

(12) (a) Golding, R. M.; Holton, M. P. *Aust. J. Chem.* **1972**, *25*, 2577. (b) Bleaney, B. *J. Magn. Reson.* **1972**, *8*, 91. (c) Reuben, J. *Ibid.* **1973**, *11*, 103.

(13) McConnell, H. M.; Robertson, R. E. *J. Chem. Phys.* **1958**, *29*, 1361.

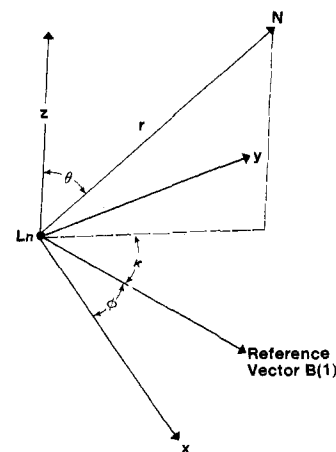


Figure 5. Coordinate system defining geometric variables r , θ , and κ for a nucleus N .

where D_1 and D_2 are the molecular susceptibility anisotropies and r , θ , and Ω are the polar coordinates of the nucleus with respect to the magnetic axes of the complex; r is the length of the vector between the paramagnetic center and the nucleus being examined, θ is the angle this vector makes with the z magnetic axis, and Ω is the angle made by the projection of the vector in the xy plane with the x magnetic axis. In the present complex the apparent C_s symmetry of the molecule fixes the z magnetic axis perpendicular to the mirror plane containing Yb , $\text{B}(1)$, $\text{B}(2)$, and $\text{B}(3)$. The magnetic xy plane coincides with this plane, and it is useful for computational purposes (vide infra) to redefine the angle Ω such that

$$\Omega = \phi + \kappa \quad (2)$$

The angles ϕ and κ are shown in Figure 5; ϕ is a magnetic parameter of the complex defining the orientation of the x magnetic axis with respect to an arbitrary reference vector and κ is a geometrical variable, the angle between the reference vector and the vector projection in the xy plane of the line joining the ytterbium to a particular nucleus in the complex. In this study we choose the $\text{Yb}-\text{B}(1)$ vector as the arbitrary reference vector. Combination of eq 1 and 2 results in an expression for the dipolar shift which involves the geometrical variables r , θ , and κ , defining the position of the nucleus and the magnetic parameters of the complex D_1 , D_2 , and ϕ . The geometrical variables r , θ , and κ were obtained from the X-ray crystallographic data with the program ORFFE and are listed in Table II. In the case of the hydrogen atoms, instead of using the X-ray positions the values of r , θ , and

(14) (a) Horrocks, W. DeW.; Fischer, R. H.; Hutchison, J. R.; LaMar, G. N. *J. Am. Chem. Soc.* **1966**, *88*, 2436. (b) Kurkland, J.; McGarvey, B. R. *J. Magn. Reson.* **1970**, *2*, 286.

Table II. Geometric Variables for Yb(HBPz₃)₃^{a,c}

nucleus	<i>r</i> , Å	θ , deg	κ , deg	$\frac{3 \cos^2 \theta - 1}{r^3}$	
				Å ⁻³ × 10 ²	Å ⁻³ × 10 ²
Hydrogen					
H(123)	3.65 (5)	24.3 (12)	62.8 (15)	3.08 (16)	0.348 (42)
H(453)	3.74 (5)	28.7 (12)	-165.9 (15)	2.51 (16)	0.441 (42)
H(783)	3.62 (5)	30.0 (12)	-65.1 (15)	2.63 (16)	0.527 (42)
H(124)	5.60 (5)	42.3 (6)	35.4 (18)	0.364 (20)	0.258 (10)
H(454)	5.68 (5)	42.4 (6)	162.6 (18)	0.347 (20)	0.249 (10)
H(784)	5.61 (5)	43.0 (6)	-97.0 (18)	0.341 (20)	0.264 (10)
H(125)	5.48 (5)	65.5 (5)	16.9 (6)	-0.295 (15)	0.504 (15)
H(455)	5.56 (5)	65.4 (5)	144.3 (6)	-0.279 (15)	0.481 (15)
H(785)	5.50 (5)	65.3 (5)	-117.4 (6)	-0.285 (15)	0.495 (15)
H(33)	3.85 (5)	<i>b</i>	-76.3 (8)	-1.76 (7)	1.76 (7)
H(63)	3.74 (5)		52.7 (8)	-1.92 (7)	1.92 (7)
H(93)	8.07 (5)		-127.2 (5)	-0.190 (4)	0.190 (4)
H(34)	5.80 (5)		-54.1 (5)	-0.513 (15)	0.513 (15)
H(64)	5.72 (5)		75.0 (5)	-0.533 (15)	0.533 (15)
H(94)	8.08 (5)		-145.9 (5)	-0.190 (4)	0.190 (4)
H(35)	5.66 (5)		-27.6 (5)	-0.551 (16)	0.551 (16)
H(65)	5.62 (5)		101.8 (5)	-0.563 (16)	0.563 (16)
H(95)	5.82 (5)		-157.6 (5)	-0.509 (12)	0.509 (12)
H(1)	4.79 (5)		1.1 (8)	-0.911 (30)	0.911 (30)
H(2)	4.80 (5)		130.3 (8)	-0.904 (30)	0.904 (30)
H(3)	3.23 (5)		-154.4 (9)	-2.96 (14)	2.96 (14)
Carbon and Boron					
C(123)	3.43 (1)	36.0 (7)	37.1 (15)	2.39 (9)	0.855 (30)
C(453)	3.52 (1)	38.3 (7)	169.9 (15)	1.94 (9)	0.881 (30)
C(783)	3.42 (1)	39.1 (7)	-91.4 (15)	2.01 (9)	0.994 (30)
C(124)	4.61 (1)	45.6 (4)	30.2 (10)	0.476 (20)	0.520 (8)
C(454)	4.68 (1)	46.2 (4)	158.6 (10)	0.427 (20)	0.508 (8)
C(784)	4.62 (1)	46.6 (4)	-101.3 (10)	0.421 (20)	0.535 (8)
C(125)	4.52 (1)	60.0 (2)	19.0 (8)	-0.271 (9)	0.811 (6)
C(455)	4.60 (1)	60.4 (2)	147.3 (8)	-0.276 (9)	0.776 (6)
C(785)	4.54 (1)	60.4 (2)	-114.3 (8)	-0.266 (9)	0.806 (6)
C(33)	3.64 (1)	<i>b</i>	-60.0 (2)	-2.08 (2)	2.08 (2)
C(63)	3.54 (1)		69.5 (2)	-2.25 (2)	2.25 (2)
C(93)	7.12 (1)		-131.0 (2)	-0.277 (1)	0.277 (1)
C(34)	4.80 (1)		-49.6 (2)	-0.904 (6)	0.904 (6)
C(64)	4.73 (1)		79.8 (2)	-0.943 (6)	0.943 (6)
C(94)	7.14 (1)		-142.0 (2)	-0.275 (1)	0.275 (1)
C(35)	4.71 (1)		-33.3 (2)	-0.955 (6)	0.955 (6)
C(65)	4.67 (1)		96.3 (2)	-0.984 (6)	0.984 (6)
C(95)	5.89 (1)		-147.0 (2)	-0.489 (3)	0.489 (3)
B(1)	3.59 (1)		0.0 (2)	-2.16 (2)	2.16 (2)
B(2)	3.60 (1)		130.0 (2)	-2.14 (2)	2.14 (2)
B(3)	3.53 (1)		-134.5 (3)	-2.28 (2)	2.28 (2)

^a Numbers in parentheses represent the estimated errors in the least significant digits. ^b Nuclei H(33) to H(3) and C(33) to B(3) are assumed to lie in the plane formed by Yb, B(1), B(2), and B(3). The value of θ for these nuclei is therefore 90.0°. ^c The three-digit numbers identify pairs of nuclei which are rendered equivalent by the molecular mirror plane, the first two numbers denote the equivalent pyrazolyl rings and the third the position of the nucleus in the ring.

κ were obtained by repositioning the hydrogen atoms with C-H and B-H bond lengths of 1.08 and 1.20 Å, respectively. The errors in the positions of the atoms are assumed to be isotropic, for the carbon and boron atoms they are taken as 0.01 Å and for the hydrogen atoms they are assumed to be 0.05 Å. The errors in *r*, θ , and κ are calculated by using these isotropic errors. When two sets of geometric variables are available for one type of nucleus, (this arises from the mirror plane being a noncrystallographic mirror plane in the X-ray structure) the average value is used and the errors are adjusted to reflect the ranges in the two sets of observed values. The observed lanthanide-induced shifts, $(\Delta\nu/\nu_0)$ LIS, are calculated from the chemical shifts in the paramagnetic complex, $(\Delta\nu/\nu_0)$ para, using the chemical shifts in the isostructural diamagnetic lutetium complex, $(\Delta\nu/\nu_0)$ dia, and eq 3. It is unfortunate that a rigorous assignment of the com-

$$\left(\frac{\Delta\nu}{\nu_0}\right)\text{LIS} = \left(\frac{\Delta\nu}{\nu_0}\right)\text{para} - \left(\frac{\Delta\nu}{\nu_0}\right)\text{dia} \quad (3)$$

Table III. Diamagnetic Reference Shifts

		range ^a	average	uncertainty
¹ H				
3-H	d(2)	7.92-6.49	7.2	±0.7
5-H	d(1)	7.79-5.18	6.5	±1.3
4-H	t(2)	6.09-6.05	6.07	±0.02
	t(1)	6.22-5.55	5.9	±0.3
BH			4.5	±0.5
¹³ C				
3-C	(2)	143.45-133.93	138.7	±4.8
5-C	(2)	105.32-104.45	104.9	±0.4
3-C	(1)	142.16-132.56	137.4	±4.8
5-C	(1)	104.45-103.36	103.9	±0.5
¹¹ B				
			-4.1	±1.0

^a Shifts in ppm taken from Table I.

Table IV. Six Sets of Magnetic Parameters Obtained from the Observed LIS of H(123), H(453), and H(783) Signals^{a,b}

soln	$D_1 \times 10^{-2}$	$D_2 \times 10^{-2}$	ϕ , deg
1	8.8	46.8	-23.3
2	11.2	63.6	33.7
3	7.4	-61.7	11.8
4	11.2	65.3	17.5
5	8.9	-47.6	-12.9
6	7.3	-59.2	39.8

^a Parameters calculated with average values of $(3 \cos^2 \theta - 1)/r^3$ and $(\sin^2 \theta)/r^3$ of $2.7 \times 10^{-2} \text{ Å}^{-3}$ and $0.44 \times 10^{-2} \text{ Å}^{-3}$ respectively (see Table II). ^b D_1 and D_2 in units of Å³/ppm.

plicated Lu(HBPz₃)₃ NMR spectra is not possible. The resonances in the ¹H spectrum can be classified into two groups based on proton-proton coupling information, the 3-H and 5-H resonances are doublets and the 4-H signals are triplets. Further classification within each group can be made from relative integrations (either 2 or 1). Similarly the ¹³C NMR spectrum can only be assigned in groups by using the large chemical shift differences between the 4-C and the 3-C, 5-C atoms which resonate in the same region, and the relative peak integrations. Within most of these assigned groups there is a range of chemical shifts and consequently an average value has to be used as the diamagnetic zero for a group of nuclei. The ranges and average values are given in Table III. The ranges are incorporated into the observed lanthanide-induced shifts as an uncertainty.

Specific assignment of the Lu(HBPz₃)₃ spectra is not essential to obtaining a fit of calculated to observed lanthanide-induced shifts for Yb(HBPz₃)₃. However, in the Yb(HBPz₃)₃ spectra each resonance must be assigned to a definite nucleus with geometrical variables, *r*, θ , and κ . The large numbers of resonances and the lack of a coupling handle (the proton-proton coupling is "washed out" by line broadening caused by the paramagnetic metal ion) makes an assignment of the ¹H NMR spectrum merely by inspection impossible. Consideration of the line widths and relative integration allows the assignment of some of the resonances into groups. The three resonances due to the three pairs of equivalent nuclei H(13)/H(23), H(43)/H(53), and H(73)/H(83) constitute one such group (these and other equivalent pairs are relabeled with three-digit numbers, H(13)/H(23) becomes H(123) and so forth). These protons are closer to the ytterbium than the others on the same pyrazolyl group by at least 1.5 Å, their NMR signals have correspondingly greater line widths¹⁵ and the resonances are easily recognizable in the spectrum. Similarly, the two resonances due to H(33) and H(63) form another group and can be readily picked out in the spectrum. The B-H protons also form a group and can be identified by their large "inhomogeneously broadened"

(15) Swift, T. J. In "NMR of Paramagnetic Molecules"; LaMar, G. N., Horrocks, W. DeW., Holm, R. H., Eds.; Academic Press: New York, 1973; p 53.

Table V. Observed and Calculated ^1H Chemical Shifts (ppm) for $\text{Yb}(\text{HBPz}_3)_3$

	chemical shift ^a	$(\frac{\Delta\nu}{\nu_0})\text{LIS}^b$	$(\frac{\Delta\nu}{\nu_0})\text{dip}^c$	$(\frac{\Delta\nu}{\nu_0})\text{LIS} - (\frac{\Delta\nu}{\nu_0})\text{dip}$
H(123)	34.8	27.6 (8)	23.2 (19)	4.4
H(453)	50.4	43.2 (8)	41.2 (24)	2.0
H(783)	10.3	3.1 (8)	3.3 (23)	-0.2
H(124)	15.3	9.15 (2)	10.3 (6)	-1.2
H(454)	15.1	9.00 (2)	9.3 (6)	-0.3
H(784)	-0.6	-6.70 (2)	-6.5 (6)	-0.2
H(125)	24.4	17.3 (8)	18.7 (10)	-1.5
H(455)	4.0	-3.2 (8)	-3.0 (9)	-0.2
H(785)	0.3	-7.0 (8)	-8.1 (9)	1.1
H(33)	-91.3	-97.8 (13)	-91.5 (34)	-6.3
H(63)	-7.3	-13.8 (13)	-10.0 (27)	-3.8
H(93)	7.2	0.7 (13)	-1.0 (13)	1.7
H(34)	-12.0	-17.9 (3)	-18.4 (6)	0.5
H(64)	-13.5	-19.4 (3)	-19.6 (6)	0.2
H(94)	10.3	4.4 (3)	3.9 (3)	0.5
H(35)	9.4	2.9 (13)	1.2 (14)	1.7
H(65)	-21.4	-27.9 (13)	-29.4 (15)	1.5
H(95)	24.1	17.6 (13)	15.7 (14)	1.9
H(1)	32.5	28.0 (8)	29.7 (15)	-1.7
H(2)	-21.0	-25.5 (8)	-27.4 (14)	1.9
H(3)	106.5	102.0 (10)	84.3 (58)	17.7

^a Shift relative to Me_4Si . Measured with internal standard CHDCl_2 , δ 5.32 ppm. ^b Calculated using eq 3 and data in Table III. ^c Numbers in parentheses after the calculated dipolar shift represent the effective variance (see ref 17) in the least significant digit.

Table VI. Magnetic Parameters from Least-Squares Refinement of Dipolar Shifts of $\text{Yb}(\text{HBPz}_3)_3$ ^a

no. and type of resonances	$D_1 \times 10^{-2}$	$D_2 \times 10^{-2}$	ϕ , deg	R_w , %
21 ^1H	8.8 (5)	43.6 (9)	-10.1 (5)	8.4
18 ^{13}C , 3 ^{11}B	8.8 (7)	42.3 (11)	-11.2 (7)	10.1
21 ^1H , 18 ^{13}C , 3 ^{11}B	8.9 (5)	42.6 (8)	-10.9 (4)	9.9

^a Weighted R factor, $R_w = (\sum w [(\Delta\nu/\nu_0)\text{LIS} - (\Delta\nu/\nu_0)\text{dip}]^2 / \sum (\Delta\nu/\nu_0)\text{LIS}^2)^{1/2}$ where $w = 1/(\sigma_{\text{eff}})^2$.

line widths. Additionally from Figure 4 it can be seen that H(3) is much closer to the ytterbium than both H(1) and H(2). Thus H(3) can be definitely assigned while H(1) and H(2) form a group. There are six ways of assigning the three resonances arising from H(123), H(453), and H(783) which lead to the six sets of values of D_1 , D_2 , and ϕ shown in Table IV. These are exact solutions of eq 1. Only one of these solutions (solution 1) gives calculated shifts which successfully account for the observed shifts for H(33), H(63), H(1), H(2), H(3), and the three ^{11}B nuclei. This solution also gave reasonable shifts for the remaining ^1H nuclei and a full assignment of the spectrum was then made by using calculated shifts from the preliminary model. Heteronuclear decoupling experiments allowed the matching of all the ^{13}C and ^{11}B resonances to the resonances of the protons to which they are directly bonded. Selective decoupling was extremely useful in the assignment of the spectra and was facilitated by the large differences in the chemical shifts of the protons and the nuclear Overhauser effect which appears to be unaffected by the presence of the paramagnetic ion. Fits of calculated to observed dipolar shifts were carried out with a weighted nonlinear least-squares¹⁶ computer program adapted to combine the uncertainties in the observed shifts and the geometric variables r , ϕ , and κ as an effective variance¹⁷ (σ_{eff}). The weight assigned to each isotropic shift is $1/(\sigma_{\text{eff}})^2$. A listing of the program is available from the authors. The values of the observed shifts, and the calculated dipolar shifts from the least-squares fit for the protons in $\text{Yb}(\text{HBPz}_3)_3$ are listed

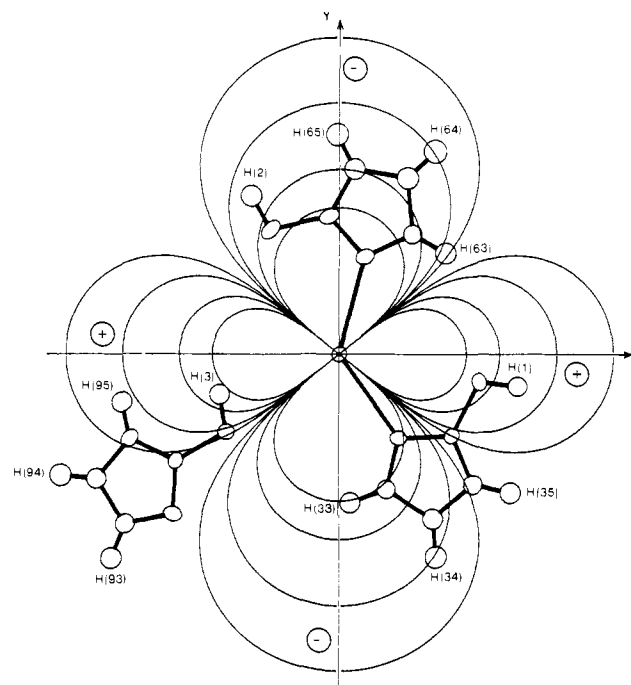


Figure 6. Contour map of ^1H dipolar shifts in $\text{Yb}(\text{HBPz}_3)_3$; contours are at ± 100 , ± 50 , ± 20 , and ± 10 ppm.

in Table V. The magnetic parameters D_1 , D_2 , and ϕ , and the reliability factor R_w from the refinement are given in Table VI. The agreement between observed and calculated shifts is good as shown by the value of 8.4% for R_w . Although three nuclei H(3), H(33), and H(63) show quite large differences between observed and calculated shifts it should be noted that the calculated shifts for these nuclei have similarly large effective variances. The goodness of fit confirms the initial assumption that the complex has the same structure in both the solid and solution states. Interestingly, 12 of the NMR unique ^1H nuclei lie in the magnetic x,y plane defined by the 3 boron atoms and the ytterbium. Figure 6 shows a map of the magnitude of the dipolar shifts in this plane and the orientation of the x axis with respect to the complex. The contours shown are for shifts ± 10 , ± 20 , ± 50 , and ± 100 ppm, which are calculated from eq 1 and the D_1 and D_2 values listed in Table VI. The view of the complex is the same as that in Figure 4 but all the atoms not in the x,y plane have been removed for clarity.

Figure 6 provides a visual description of the sensitivity of the various nuclei to small changes in their positions, particularly H(3) and H(33) which lie in regions of high shift and H(63) and B(3) which lie close to the nodal surface.

Figure 6 is also useful in determining the conformation adopted by the bidentate ligand in solution. The six-membered metal chelate ring, which is in the boat conformation in the solid state, may be undergoing a "ring flip" process, which has ample precedent in complexes containing bidentate polypyrazolylborate ligands,¹⁸ or may favor the other boat conformation, in solution. Additionally rotation of the uncoordinated pyrazolyl group N(91)...C(95) about the N(91)-B(3) bond is also possible. Examination of the observed and calculated shifts of protons H(3) and H(95) of the uncoordinated pyrazolyl group, in conjunction with the dipolar surface map of Figure 6 indicates that the boat conformation found in the crystal structure is maintained in solution and that the uncoordinated pyrazolyl group is similarly locked into the rotational conformation seen in the X-ray structure. The observed LIS for H(3) is already 18 ppm further downfield than the value calculated by the structural model. Any movement away from the particular boat conformation observed would change the position of H(3) such that the calculated shift for the

(16) Marguadt, D. W. *J. Soc. Ind. Appl. Math.* 1963, 11, 431.

(17) Baiker, D. R.; Diana, L. M. *A.J.P.* 1974, 42, 224.

(18) Shaver, A. *J. Organomet. Chem. Libr.* 1971, 3, 157 and references therein.

Table VII. Observed LIS and Calculated Dipolar ^{13}C and ^{11}B Chemical Shifts (ppm) for $\text{Yb}(\text{HBPz}_3)_3$

	chemical shift ^a	$(\frac{\Delta\nu}{\nu_0})_{\text{LIS}}^b$	$(\frac{\Delta\nu}{\nu_0})_{\text{dip}}^c$	$(\frac{\Delta\nu}{\nu_0})_{\text{LIS}} - (\frac{\Delta\nu}{\nu_0})_{\text{dip}}$
C(123)	184.4	45.7 (48)	43.5 (52)	2.2
C(453)	183.3	44.6 (48)	44.6 (51)	0.0
C(783)	123.0	-15.7 (48)	-20.4 (51)	4.7
C(124)	121.2	16.3 (4)	21.6 (7)	-5.3
C(454)	114.0	9.1 (4)	14.4 (7)	-5.3
C(784)	90.9	-14.0 (4)	-12.3 (8)	-1.7
C(125)	164.7	26.0 (48)	29.7 (8)	-3.7
C(455)	135.9	-2.8 (48)	-1.1 (49)	-1.7
C(785)	123.0	-15.7 (48)	-13.5 (49)	-2.2
C(33)	56.1	-81.3 (48)	-88.2 (49)	6.9
C(63)	71.0	-66.4 (48)	-62.8 (49)	-3.6
C(93)	142.7	5.3 (48)	0.5 (48)	4.8
C(34)	74.4	-29.5 (5)	-28.0 (6)	-1.5
C(64)	63.0	-40.9 (5)	-37.7 (6)	-3.2
C(94)	109.1	5.2 (5)	4.5 (5)	0.7
C(35)	129.8	-7.6 (48)	-7.7 (48)	0.1
C(65)	89.4	-48.0 (48)	-49.8 (48)	1.8
C(95)	148.4	11.0 (48)	10.7 (48)	0.3
B(1)	57.7	61.8 (10)	65.7 (13)	-3.9
B(2)	-69.1	-65.0 (10)	-67.4 (12)	2.4
B(3)	16.3	20.4 (10)	15.0 (14)	5.4

^a Shifts in ppm relative to Me_4Si or BF_3OEt_2 . ^{13}C shifts measured with internal standard CH_2Cl_2 δ 53.8 ppm. ^b Calculated with equation 3 and data in Table III. ^c Number in parentheses after the calculated pseudocontact shift represents the effective variance (see reference 17) in the least significant digit.

new position would be even smaller than the presently calculated shifts. By similar argument it can be seen from Figure 6 that rotation of the free pyrazolyl group away from the solid-state conformation would result in a new position for H(95) which would have a much smaller dipolar shift.

Of note is the orientation of the x magnetic axis. The value of ϕ from the least-squares refinement is -10.1° while the angle between the reference $\text{Yb}-\text{B}(1)$ vector and the plane $\text{Yb}-\text{N}(12)-\text{N}(22)$ is -20.1° . The coordination polyhedron of $\text{Yb}(\text{HBPz}_3)_3$ formed by the eight ligating nitrogen atoms is of bi-capped-trigonal-prismatic geometry with approximate C_{2v} symmetry,² the $\text{Yb}-\text{N}(12)-\text{N}(22)$ plane containing the pseudo-2-fold rotation axis. Thus it is gratifying to see that the x magnetic axis lies close to the pseudo-2-fold axis where it would necessarily be fixed if the coordination polyhedron possessed rigorous C_{2v} symmetry.

The good agreement between calculated and observed shifts demonstrates that there is no detectable contribution to the lanthanide-induced proton shifts in the present complex from a Fermi contact mechanism. This result is not remarkable. Consideration of the lanthanide ion dependent parameters, which determine the relative magnitude of contact and dipolar shifts, indicates that $\text{Yb}(\text{III})$ should exhibit the smallest relative contact shifts¹² and this has led several investigators¹⁹ to successfully ignore contact contributions when using $\text{Yb}(\text{III})$ as a structural probe. This work provides further evidence in support of this often made assumption.²⁰

(19) (a) Agresti, D. G.; Lenkinski, R. E.; Glickson, J. D. *Biochem. Biophys. Res. Commun.* **1977**, *76*, 711. (b) Lee, L.; Sykes, B. D. *Biophys. J.* **1980**, *32*, 193.

There is experimental evidence that the ^{17}O and ^{14}N chemical shifts in lanthanide complexes are dominated by the Fermi contact mechanism,²³ and theory also predicts that the contact shifts for these and ^{11}B nuclei should be greater than for the ^1H nucleus.²⁴ Table VII contains the observed shifts for the 18 ^{13}C and 3 ^{11}B nuclei in the complex together with the calculated shifts from a least-squares refinement. The value of D_1 , D_2 , and ϕ from this refinement and those from a refinement with 21 ^1H , 18 ^{13}C and 3 ^{11}B nuclei are contained in Table VI. The close agreement between the observed shifts and calculated dipolar shifts indicates that the contact contributions to the ^{13}C and ^{11}B lanthanide-induced shifts are so small as to be essentially undetectable in the present analysis of the $\text{Yb}(\text{HBPz}_3)_3$ system. However, it should be noted that although the shifts are adequately accounted for solely by a dipolar mechanism, the rather large uncertainties in the observed lanthanide-induced shifts for some ^{13}C nuclei (up to 5 ppm) make it difficult to completely rule out a small contact contribution to the ^{13}C shifts.

Conclusion

The known solid-state structure and the unexpected rigid solution behavior of $\text{Yb}(\text{HBPz}_3)_3$ have provided an unparalleled opportunity for detailed analysis of its ^1H , ^{13}C , and ^{11}B NMR spectra. The nonaxial symmetry of the molecule clearly necessitates the use of the full two-term dipolar equation. The close agreement between the calculated shifts on the basis of this equation and the experimentally observed lanthanide-induced shifts not only shows that the solid-state structure remains unchanged upon dissolution, but that, at least for this lanthanide ion and in particular for the proton shifts, contact contributions to the induced shifts are negligible. Although a preliminary knowledge of the solid-state structure was necessary to deduce the solution structure of the present complex, the success of the approach and the characteristics of the $\text{Ln}(\text{HBPz}_3)_3$ complexes have important ramifications. As an obvious extension we will show²² that the solution structure of $\text{Yb}(\text{HBPz}_3)_3$ can be used directly to account, via the dipolar shift mechanism, for the ^1H NMR spectra of other $\text{Ln}(\text{HBPz}_3)_3$ ($\text{Ln} = \text{Tm}, \text{Er}, \text{Ho}, \text{Dy}$) complexes and that for these complexes a satisfactory separation of contact from dipolar contributions is possible for the ^{13}C and ^{11}B lanthanide-induced shifts. More intriguing is the possibility that derivatives of $\text{Ln}(\text{HBPz}_3)_3$ may serve as rigid and therefore rigorously calculable lanthanide probes for solution structural studies, and the feasibility of this is being evaluated.

Acknowledgment. We thank the Natural Sciences and Engineering Research Council (NSERC A6659 to JT) and the University of Alberta for financial support of this research. We are also grateful to Professor R. E. D. McClung for help with the computing and many helpful discussions and to Glen Bigam for recording the NMR spectra.

(20) It has been shown²¹ that the lanthanide-induced proton shifts are in general dominated by dipolar contributions. We will show²² that this is true for other $\text{Ln}(\text{HBPz}_3)_3$ complexes as long as the full two-term expression, eq 1, is used to calculate LIS.

(21) (a) Cramer, R. E.; Dubois, R.; Seff, K. *J. Am. Chem. Soc.* **1974**, *96*, 4125. (b) Horrocks, W. DeW.; Sipe, J. P., III *Science (Washington, D.C.)* **1972**, *177*, 994.

(22) Stainer, M. V. R.; Takats, J., manuscript in preparation.

(23) (a) Reuben, J.; Fiat, D. *J. Chem. Phys.* **1969**, *4909*. (b) Witanowski, M.; Stefaniak, L.; Januszewski, H. *J. Chem. Soc., Chem. Commun.* **1971**, 1573.

(24) McGarvey, B. R.; Kurkland, R. J. In "NMR of Paramagnetic Molecules"; LaMar, G. N., Horrocks, W. DeW., Holm, R. H., Eds.; Academic Press: New York, 1973; p 559.